Assessment of the Impacts of the 2023 Earthquake in Diyarbakir, Turkey with CBERS-4A Satellite Images

Bruno G. Miranda[1], Felipe de O. Passos[1], Gabriel Dietzsch[1], Ocione D. N. Filho[1], Tiffany L. J. T. de Mendonça[1], Thales S. Korting[1], Laércio Massaru Namikawa[1], Douglas F. M. Gherardi[1], Luciano P. Pezzi[1], Gilberto R. Queiroz[1]

Instituto Nacional de Pesquisas Espaciais – (INPE)
Av. dos Astronautas – n° 1758 – Jardim da Granja,
São José dos Campos - SP – CEP 12227-010.

{bruno.miranda, ocione.filho, tiffany.mendonca}@inpe.br
{thales.khorting, laercio.namikawa, luciano.pezzi,
douglas.gherardi, gilberto.queiroz}@inpe.br
dietzschgd@fab.mil.br, felipeo.passos@gmail.com

1

Abstract. *This study aims to identify buildings damaged by the earthquake of 02/06/2023 in the city of Diyarbakir (Turkey) using images from the CBERS-4A satellite. The images were processed in Python in order to compare the images from before (2021) and after (2023) the earthquake. Statistical measures such as mean, standard deviation, and entropy were used to analyze the results. The buildings layer Open Street Maps was also used to identify the polygons and areas affected by the disaster. By combining these techniques, it was possible to identify areas that showed changes after the earthquake.*

Resumo. *Este estudo visa identificar construções danificadas pelo terremoto de 06/02/2023 na cidade de Diyarbakir (Turquia) a partir de imagens do satélite CBERS-4A. As imagens foram processadoas no Python para ser feita uma comparação das imagens de antes (2021) e depois (2023) do terremoto. Foram realizadas, medidas estatísticas como média, desvio padrão e entropia para a análise dos resultados. Foi usado também a camada buildings do Open Street Maps para identificar os polígonos e áreas afetadas pelo desastre. Através da combinação dessas técnicas, foi possível identificar áreas que sofreram mudanças após a ocorrencia do terremoto.*

1. Introduction

The earth's environment is constantly being transformed, whether by anthropogenic or natural changes. Some natural physical processes are capable of generating drastic changes in the earth's surface, such as earthquakes, hurricanes, and volcanic eruptions. When natural processes impact a social system, causing serious damage that exceeds an individual's ability to cope with the impact, a natural disaster occurs [Tobin and Montz 1997].

In February 2023, news of an earthquake in Turkey and Syria impacted the world. The United States Geological Survey (USGS) recorded an earthquake in southeastern Turkey at a depth of 24 kilometers. The catastrophe caused more than 50,000 victims and is considered the biggest earthquake in the region in the last 20 years, according to Turkey's Presidency of Emergencies and Disasters (AFAD). The city of Diyarbakir, in the south-east of Turkey, was one of those affected, as shown in figure 1. Southeast Turkey is located between the Arabian and Eurasian tectonic plates and is a constant target for tremors, but the number of tremors in the region has increased significantly in 2023 [AFAD 2023].

Figura 1. Earthquake damage in the city of Diyarbakir, Turkey in February 2023.
Font: Sertac Kayar.

One way of monitoring such events is through the use of satellites. Remote sensing provides information on these areas in a short space of time, making it a fundamental tool for managing these disasters. Brazil has the CBERS (China-Brazil Earth Resources Satellite) program, a partnership between Brazil and China that makes satellite images available for free, helping to spread the beneficial use of these images around the world.

[Voigt et al. 2007] states the effectiveness of the techniques used to monitor earthquakes, whether using thermal infrared images [Andrew et al. 2002]; [Ouzounov et al. 2006]; [Joyce et al. 2009], or In-SAR (Interferometric Synthetic Aperture Radar) images to identify the deformation of the earth's surface [Gabriel et al. 1989] and [Massonnet et al. 1993]. According to [Dong and Shan 2013], optical images are excellent for identifying areas affected by an earthquake, as they are easy to interpret.

Therefore, the aim of this work is to analyze the area affected by the earthquake in the city of Diyarbakir and identify the damaged buildings using images taken by the CBERS-4A satellite. Analysis of the images will enable the affected buildings to be identified.

2. Materials and Methods

2.1. Materials

The following libraries from *Python* programming language were used in this work: *rasterio*, *matplotlib numpy*, *gdal*, *osmnx* and *geopandas*. *Quantum Geographic Information System (QGis)* software was also used to manipulate the images.

2.2. Methods

The work methodology is presented in the flowchart illustrated below (Figure 2).

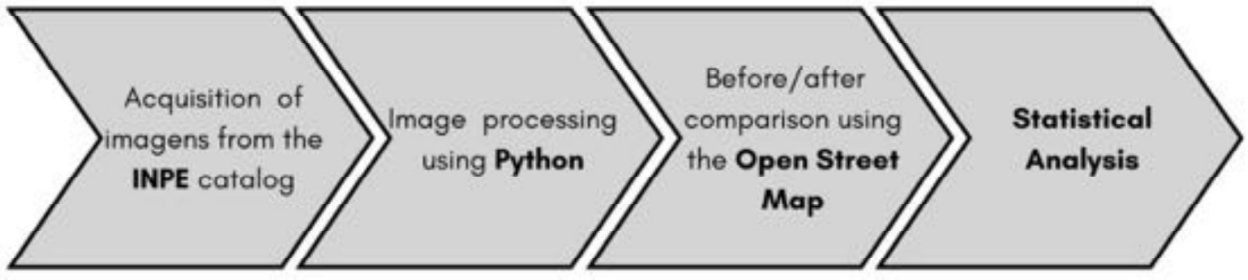

Figura 2. Flowchart of the methodology used in the study to compare the impact of the earthquake in Turkey.

This study uses images acquired by the Panchromatic sensor of the CBERS4A satellite, captured at different times - before (May 14, 2021) and after (February 14, 2023) a seismic event. These images were obtained from the [INPE 2023] image catalog and are available on the International Charter for Space and Major Disasters, a global satellite reprogramming initiative to which the National Institute for Space Research (INPE) is associated.

QGIS software was used to crop the images in a standardized way, using the *rasterio* and *matplotlib* libraries in the *GoogleColab* environment to load and verify georeferencing information, prioritizing band 1, since it has better conditions for consistent analysis. The GDAL library was used to extract maximum and minimum pixel values, normalizing grey levels and applying advanced contrast enhancement techniques, particularly in areas of interest affected by the earthquake.

The *buildings* layer was added in QGIS, incorporating vector data of the buildings. Information from the *OpenStreetMap* was integrated to delimit the areas of the buildings by creating polygons. An analytical process was developed, involving the creation of lists to store polygon indices and pixel averages, with the execution of clipping and statistical operations.

The statistical analyses used were:

- **Mean:** First, the mean of the values inserted in each pixel was calculated for the different polygons of the buildings layer in the before and after images. The absolute difference between the means obtained for the before and after images was used to detect changes, with a criterion factor for values greater than or equal to 30. As a result of this analysis, 20 values were found that showed changes possibly caused by the earthquake in the region, some of which were clearly visible in the CBERS-4A images.

- **Entropy:** To calculate entropy, the methodology used was that of [Shannon 1948] and described in more detail by [Nascimento and Prudente 2016]. Similarly, the average was computed for the values for the two images, but with a criterion factor of 0.5 for the classification of the absolute difference. As a result of this analysis, 368 values were found that showed changes.

- **Standard Deviation:** The procedure for calculating the standard deviation is similar to that used for the mean. The criterion factor for classifying the absolute difference in this case was 20. As a result of this analysis, 45 values were found that showed changes.

The results were displayed, and significant changes related to the earthquake were identified based on the established criteria. Entropy and standard deviation alerts were generated for the filtered polygons, providing useful information on the changes occurring in the areas affected by the earthquake.

3. Results

Figure 3 shows that they have different brightnesses and contrasts, which can make visual analysis difficult. Therefore, the comparison of the before (2021) image with the 2023 (after) image must be refined, i.e. the 2021 image requires a definition of the band to be used for comparison with the Panchromatic band of the after image. Thus, Bands 1 to 4 are plotted below in Figure 4 to define which has better quality and contrast to make it possible to identify changes caused by the earthquake and will be used for the analyses.

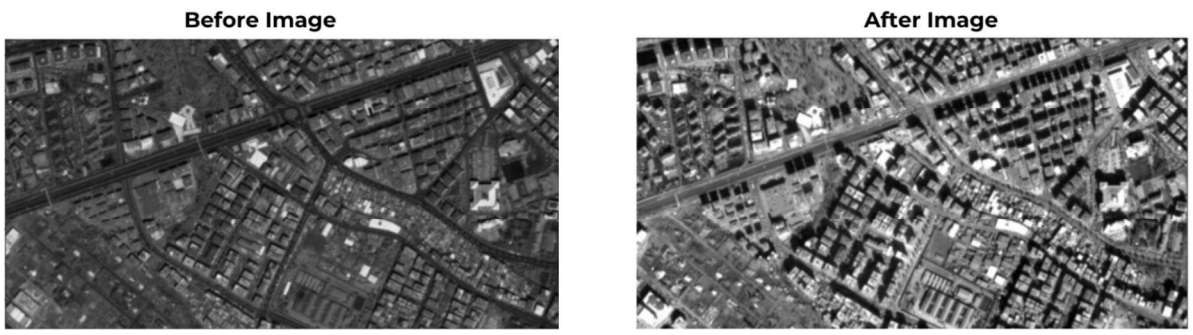

Figura 3. Images of the differences in brightness and contrast between bands 1 (left) and 4 (right) of the CBERS-4A satellite image from 2021.

Figura 4. Brightness and contrast differences between bands 1 and 4 of the CBERS-4A satellite for the 2021 image (before the earthquake). Possibilita

After visual analysis, it was possible to detect that Band 1 proved to be the sharpest. This band corresponds to the visible blue spectrum, imaging wavelengths in the 0.45 to 0.52 µm range, with a resolution of 8 meters.

Next, the grey levels of the images were normalized to define equal scales and compare the mean, standard deviation, and entropy to obtain consistent results. To do this, the following formula was used:

$$band_{normalized} = \left(\frac{band1 - band1_{value_{min}}}{band1_{value_{max}} - band1_{value_{min}}} \right) * 255 \quad (1)$$

With the normalization, the scales for the before and after images remained at [2 - 255] and [1 - 255], respectively. The distribution of gray levels can be seen in the histogram in Figure 5.

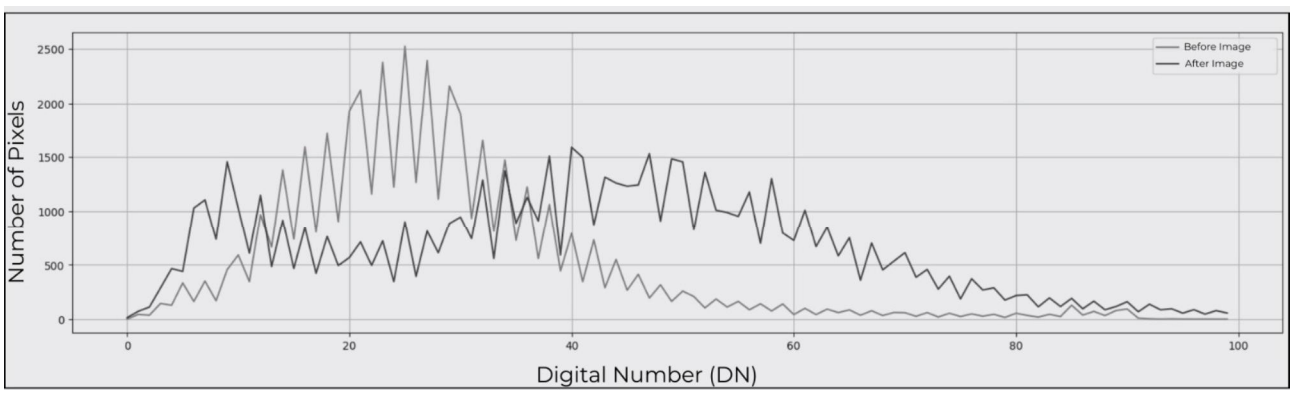

Figura 5. Normalized Histogram. The light gray line represents the distribution of gray levels in the pre-earthquake image, and the dark gray line represents the distribution of digital numbers in the post-earthquake image.

Looking at the images resulting from the normalization of the grey levels, it was necessary to improve the contrast of the 2021 image, using a gain factor of 1.5. The result of the image with improved contrast (2021) and that of 2023, together with the final histogram, are shown in Figures 6 and 7, respectively.

Figura 6. Before and After Images - Contrast. Representation of contrast in pre- and post-earthquake images.

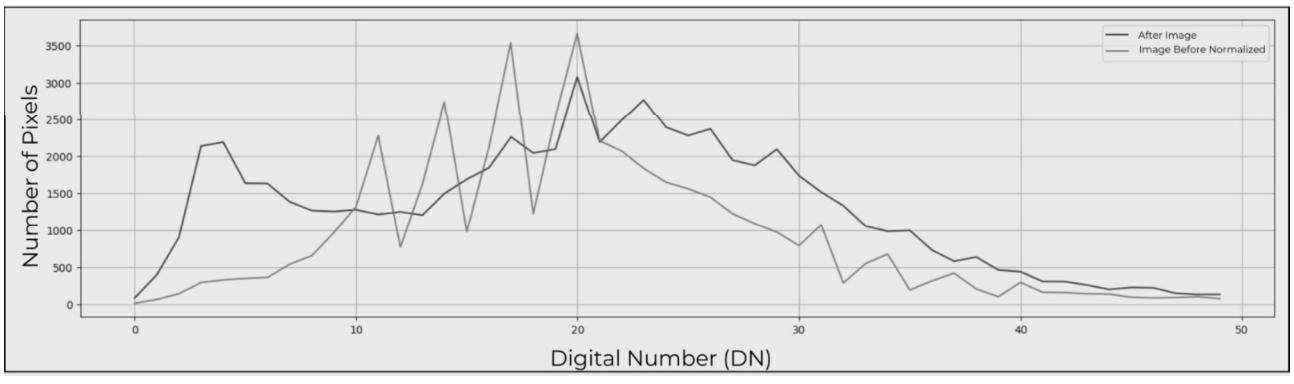

Figura 7. Contrast histogram. The light gray line represents the contrast of the pre-earthquake image, and the dark gray line represents the contrast of the post-earthquake image.

The *buildings* layer of the *Open Street Maps* was used to detect changes caused by the disaster. This layer was obtained via QGis and its *shapefile* is inserted into Figure 8, in which it shows the polygons identified as buildings (black shapes) in the study area.

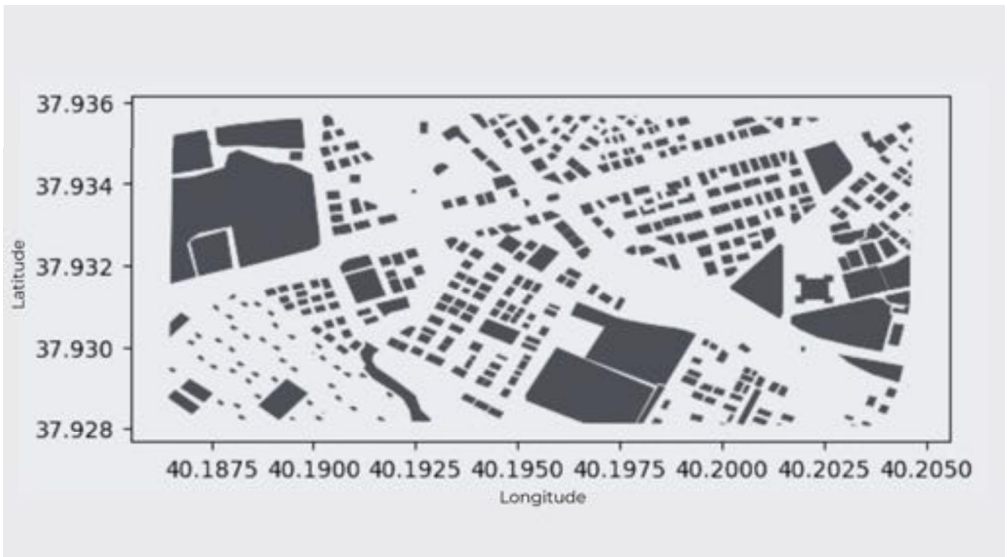

Figura 8. Shapefile Layer Buildings Open Street Maps for the Study region, the polygons indicate areas identified as buildings.

The comparison of the images from before and after the disaster was carried out as follows: the polygons were "scanned" in such a way that two lists were created: one containing the index of each *.shp* and the other containing the statistics of the pixel values read from the image. These lists will be used to carry out statistical analyses such as mean, standard deviation, and entropy to identify changes caused by the earthquake in the region.

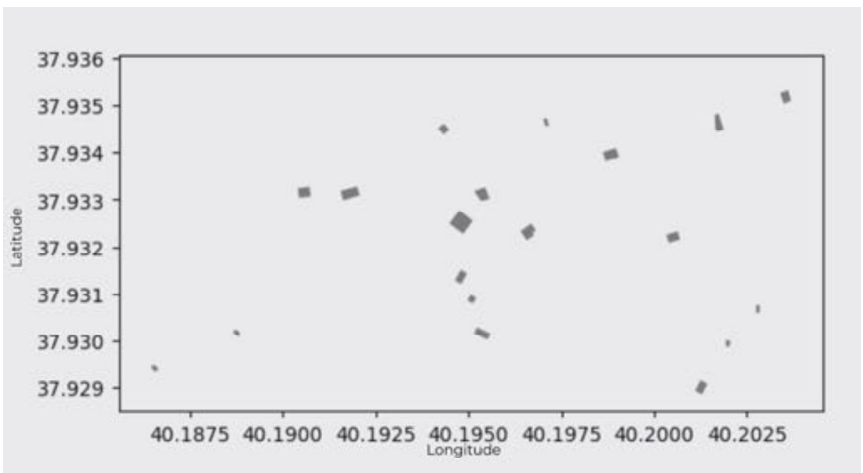

Figura 9. Shapefile of Detected Changes - Image 2023. The polygons represent the detected changes after the earthquake.

Based on the 3 measurements made (mean, entropy, and standard deviation), a procedure was carried out to detect the *shapefiles* with changes in common for all the statistics. The mean indicated changes in 20 polygons, the standard deviation 45, and the entropy indicated 368 values, resulting in 19 polygons in common. Therefore, the polygons that showed differences were selected and plotted in a new resulting shapefile so that visual identification could be done with the satellite images of the affected areas, which are shown in Figure 9. Finally, the *shapefile* generated in Figure 9 is overlaid with the post-earthquake image (2023) so that the areas affected by the earthquake disaster in Turkey can be mapped (Figure 10).

Figura 10. Shapefile Layer Buildings - Detected Changes. The polygons highlighted in the image represent the buildings that were identified as detected changes after the earthquake.

4. Conclusions

Based on all the above, it can be said that the methods used in this work to analyze the impact of the damage caused by the earthquake in Turkey were sufficient to identify the most affected locations, where some of the buildings in the city of Diyarbakir collapsed. Therefore, the conditions of the images and the sensor used were adequate to meet the objectives of this work.

Although the results were satisfactory, some problems were identified. In the before and after images, although obtained by the same sensor, there are differences in shading, sharpness, and contrast, which may have caused occasional false contours. However, given that the objective of the work was to identify buildings affected by earthquakes, only the polygons of the roofs of the targets were used, and the analysis was not impaired. The quality of the results depends on the type of sensor used and the quality of the spatial resolution of the image used; the higher the resolution, the better the image quality and the ability to identify differences.

An issue was identified when using the ”buildings”layer, the image returned not only polygons of buildings but also polygons of large areas such as fields, squares, and intersections. It would be possible to apply filtering, however, there was a risk of losing essential information about the desired targets. Taking into account the fact that these areas do not interfere with the study, this filtering was not carried out.

After processing the images, we were able to identify the areas with building damage by using the difference in the spectral response of the targets, calculated using three different techniques, obtaining more reliable results. The use of these techniques made it possible to identify damage that would have been imperceptible to the human eyes but became evident by overlaying the real image with the polygons, which made it possible to identify changes in 19 different buildings.

Referências

AFAD, D. E. M. A. (2023). Site oficial afad. https://en.afad.gov.tr/about-us, acesso em: 15 de maio de 2023.

Andrew, A. T., Mashashi, H., and Oleg, A. M. (2002). Thermal ir satellite data application for earthquake research in japan and china. *Journal of Geodynamics*, pages 33(4–5):519–534.

Dong, L. and Shan, J. (2013). A comprehensive review of earthquake-induced building damage detection with remote sensing techniques. *ISPRS Journal of Photogrammetry and Remote Sensing*, 84:85–99.

Gabriel, A. K., Goldstein, R. M., and Zebker, H. A. (1989). Mapping small elevation change sover large areas: differential radar interferometry. *Journal of Geophysical Research*, page 94:9183–9191.

INPE, I. N. P. E. (2023). Catálogo de imagens. http://www.dgi.inpe.br/catalogo/explore, acesso em: 22 maio 2023.

Joyce, K., Belliss, S., Samsonov, S., McNeill, S., and Glassey, P. (2009). A review of the status of satellite remote sensing and image processing techniques for mapping natural hazards and disasters. *Progress in Physical Geography*, 33:183–207.

Massonnet, D., Rossi, M., Carmona-Moreno, C., Adragna, F., Peltzer, G., Feigl, K., and Rabaute, T. (1993). The displacement field of the landers earthquake mapped by radar interferometry. *Nature*, 364:138–142.

Nascimento, W. and Prudente, F. (2016). Study of shannon entropy in the context of quantum mechanics: An application to free and confined harmonic oscillator. *Química Nova*, 39.

Ouzounov, D., Bryant, N., Logan, T., Pulinets, S., and Taylor, P. (2006). Satellite thermal ir phenomena associated with some of the major earthquakes in 1999–2003. *Physics and Chemistry of the Earth, Parts A/B/C*, 31:154–163.

Shannon, C. E. (1948). A mathematical theory of communication. *The Bell System Technical Journal.*, pages 27:379–423,623–656.

Tobin, G. A. and Montz, B. E. (1997). Natural hazards: explanation and investigation. *New York: The Guilford Press.*, page 388.

Voigt, S., Kemper, T., Riedlinger, T., Kiefl, R., Scholte, K., and Mehl, H. (2007). Satellite image analysis for disaster and crisis-management support. *IEEE T. Geoscience and Remote Sensing*, 45:1520–1528.